Engineered Point Spread Function of Fresnel lenses for passive infrared motion sensors

Giuseppe A. Cirino[1], Robson Barcellos[1], Luiz G. Neto[2]

1 HoloPhotonics Equipamentos Óticos e Eletrônicos Ltda-ME, Brazil
2 EESC – Department of Electrical Engineering, São Paulo University, Brazil

Address
giuseppe@holophotonics.com.br

Abstract

In this work an engineered point spread function (PSF) is applied in the design of inexpensive Fresnel lens arrays for passive infrared motion sensors. The resulting lenses have a cubic-phase distribution enabling it to distinguish the presence of humans from pets by the employment of the so-called wavefront coding method. The cubic-phase distribution used in the design can also reduce the optical aberrations present on the system. This aberration control allows a high tolerance in the fabrication of the lenses and in the alignment errors of the sensor.

Introduction

Passive infrared (PIR) motion sensors have been extensively used in homeland and corporative electronic security applications [1]. The principle of operation of this device is based on the employment of a pyroelectric detector, which is responsible for transducing the incident IR radiation into an electrical signal. This signal is amplified and filtered, generating another signal to an alarm element. To avoid false detections due to temperature variation, the pyroelectric detector presents a dual active region, with reverse polarization with respect to each other. Associated with the photo detector and the circuitry, there is a Fresnel lens array, which monitors different spatial zones and concentrate the IR radiation from a body that moves within the monitoring volume. In this case, the lens array is designed only to make sure that the incident IR radiation is concentrated on the pyroelectric detector surface, regardless the formation of a good quality image. Figure 1a shows the photography of a typical low cost passive infrared (PIR) pyroelectric motion sensor. When a human corporal mass (here called by target mass) moves through the volumetric monitoring field of the sensor, different Fresnel lenses of the array focus the IR radiation on the pyroelectric detector, generating an electrical signal at the pyroelectric detector output. Whenever electrical signal is present at the output of the pyroelectric detector, meaning that an intruder has been detected, the sensor will trip, as shown in figure 1b. The electrical current, I, in the pyroelectric detector is proportional to the rate of change in time of the temperature of the target, dT/dt, the pyroelectric coefficient of the detector, $p(t)$, and detector electrode area, A:

$$I = p(t)A\frac{dT}{dt} \tag{1}$$

Figure 1c shows the photography of a Fresnel lens array typically employed in IR motion sensor applications. This array presents 24 detection zones, with 3 sets of lenses that monitor 3 different distance fields: a near field (typically 1-2 meters from the sensor), a medium distance field (typically 3-6 meters from the sensor), and a far field (typically 8-15 meters from the sensor).

Theory of Aberration Invariance

An incoherent imaging system is linear in intensity and its point spread function (PSF), is the squared magnitude of the amplitude impulse response $h(x_i,y_i)$ [8]. The variables x_i and y_i are the coordinates in the image plane. The optical transfer function (OTF) $H(u,v)$ of the system can be defined from $h(x_i,y_i)$ by

$$H(u,v) = \frac{\int_{-\infty}^{+\infty}\int \left|h(x_i,y_i)\right|^2 \exp\left[-j2\pi\left(x_i u + y_i v\right)\right]dxdy}{\int_{-\infty}^{+\infty}\int \left|h(x_i,y_i)\right|^2 dxdy} \tag{2}$$

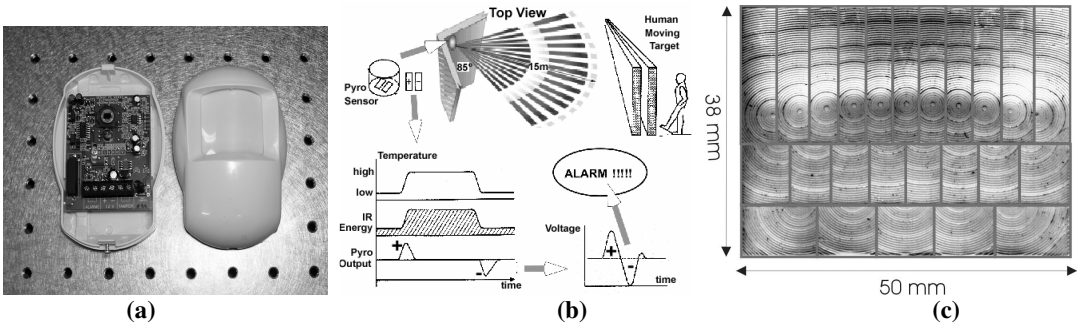

Figure 1: (a) Typical low-cost passive infrared (PIR) motion sensor; (b) schematic view of the principle of a PIR sensor. Whenever a human corporal mass (target mass) moves through the monitoring volume field, an electrical signal at the pyroelectric detector output is generated, enabling the sensor to trip; (c) photography of a Fresnel lens array typically used in PIR sensors. Each lens is delimited by a rectangle.

When an imaging system is diffraction limited, the amplitude point spread function is obtained from the Fraunhofer diffraction pattern of the exit pupil $P(x_p,y_p)$, with $P(x_p,y_p)$=1 in the region of the exit pupil and $P(x_p,y_p)$=0 outside. The variables x_p and y_p are the coordinates in the pupil plane. For aberrated imaging systems, the aberrations can be directly included in the plane of the exit pupil [8]. The phase errors in the plane (x_p,y_p) of the exit pupil is represented by $kW(x_p,y_p)$, where $k=2\pi/\lambda$ and W is the effective path-length error. The complex amplitude transmittance $P(x_p,y_p)$ in the exit pupil is given by:

$$P(x_p, y_p) = P(x_p, y_p)\exp\left[jkW(x_p, y_p)\right] \tag{3}$$

The complex function $\mathbf{P}(x_p,y_p)$ may be referred as the generalized pupil function. The PSF of an aberrated incoherent system is simply the squared magnitude of the Fraunhofer diffraction pattern of an aperture with amplitude transmittance $\mathbf{P}(x_p,y_p)$. The most common approach to obtain a focus-invariant incoherent optical imaging system is to stop down the pupil aperture or to employ an optical power absorbing apodizer, with possible π phase variations. The aperture can be viewed as an absorptive mask in the pupil plane of an optical imaging system. Although these methods increase the amount of depth of field, there is a loss in optical power at the image plane and the reduction of the diffraction-limited image resolution [2,5,8]. A non-absorptive separable cubic phase mask can be included in the exit pupil to produce an optical PSF that is highly invariant to misfocus [2,5]. Considering the cubic phase distribution, the PSF is not directly comparable to that produced from a diffraction-limited system PSF. However, because the new OTF has no regions of zeros, digital processing can be used to restore the sampled intermediate image. If the PSF is insensitive to misfocus, all values of misfocus can be restored through a single, fixed, digital filter. This combined optical/digital system produces a PSF that is comparable to that of the diffraction limited system PSF, but over a far larger region of focus. The phase cubic distribution necessary to produce this focus-invariance is described by equation 4:

$$P(x_p, y_p) = \exp\left[j20\pi\left(x_p{}^3 + y_p{}^3\right)\right] \tag{4}$$

When a focusing error is present, the center of curvature of the spherical wavefront converges towards the image of an object point source at the left or at the right of the image plane, located at the distance z_i from the exit pupil [8]. The misfocus in the generalized pupil function $\mathbf{P}(x_p,y_p)$ for an image located at the arbitrary distance z_a from the exit pupil results in the equation 5:

$$P(x_p, y_p) = P(x_p, y_p)\exp\left[\, jk\,\frac{1}{2}\left(\frac{1}{z_a} - \frac{1}{z_i}\right)\left(x_p{}^2 + y_p{}^2\right)\right] \tag{5}$$

The amplitude impulse response $h(x_i,y_i)$ of this new lens is calculated by the equation 6:

$$\mathrm{h}(\mathrm{x_i}, \mathrm{y_i}) = \int_{-\infty}^{+\infty}\int \exp\left[\mathrm{j20\pi}\left(\mathrm{x_p}^3 + \mathrm{y_p}^3\right)\right]\exp\left[\,\mathrm{jk}\,\frac{1}{2}\left(\frac{1}{\mathrm{z_a}} - \frac{1}{\mathrm{z_i}}\right)\left(\mathrm{x_p}^2 + \mathrm{y_p}^2\right)\right]\exp\left[-\,\mathrm{j2\pi}\left(\mathrm{x_p x_i} + \mathrm{y_p y_i}\right)\right]\mathrm{dx_i dy_i} \tag{6}$$

Figure 2 compares the image of the PSF for z_i=z_a=50 mm and for z_i=50 mm and z_a=70 mm. The cubic phase distribution generates a constant PSF over a far larger region of focus, compared to conventional image system. The intensity distribution of the intermediate images of the PSF remains constant for different image planes.

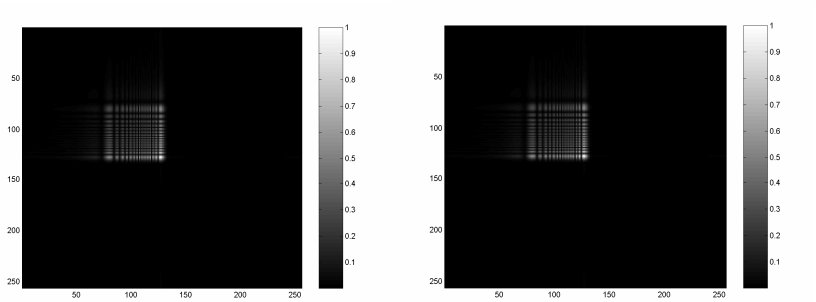

(a) **(b)**

Figure 2: (a) Image of the PSF for z_i=z_a=50 mm; (b) Image for z_i=50 mm and z_a=70 mm. The cubic phase distribution generates a constant PSF over a large region of focus.

These results are calculated using the relation:

$$\mathrm{G_i(u,v)} = H(\mathrm{u,v})\mathrm{G_g(u,v)} \tag{7}$$

The OTF *H(u,v)* of the system is calculated using equation 2. The frequency spectra of *Ig*, the input image, and *Ii*, the output image are defined by:

$$G_g(u,v) = \frac{\int_{-\infty}^{+\infty}\int I_g(x_g,y_g)\exp\left[-j2\pi\left(x_g u + y_g v\right)\right]dx_g dy_g}{\int_{-\infty}^{+\infty}\int I_g(x_g,y_g)dx_g dy_g} \tag{8}$$

$$G_i(u,v) = \frac{\int_{-\infty}^{+\infty}\int I_i(x_i,y_i)\exp\left[-j2\pi\left(x_i u + y_i v\right)\right]dx_i dy_i}{\int_{-\infty}^{+\infty}\int I_i(x_i,y_i)dx_i dy_i} \tag{9}$$

As shown in figure 2, cubic phase optical systems are insensitive to misfocus. Because the new OTF has no regions of zeros, the original images can be recovered from the focus invariant images after simple digital filtering using equation 10, as desired [2].

$$G_g(u,v) = G_i(u,v) / H(u,v) \tag{10}$$

Application of cubic phase distribution in passive infrared motion sensors

As stated above, in PIR sensors the lens array is used to concentrate the infrared radiation over the detector and not to generate an image. Regular lenses do not distinguish the presence of humans from pets. In order to assure this distinction, the cubic phase distribution is added to the regular (quadratic phase) lenses, introducing the wavefront coding in the system. In our application, the new lenses are used as a spatial filter rather than as an imaging system. When a target mass is moving through the volumetric monitoring field of the sensor, i.e., through the fileld of view of different segmented Fresnel lenses, the generated distribution of energy also moves over the detector surface. The goal is to introduce a spatial filtering that helps in the distinction between the patterns generated by a human and a pet body. This is done by using the $P_V(x_p,y_p)$ phase distribution [2-7]:

$$P_V(x_p,y_p) = \exp\left[j20\pi.y_p^{\,3}\right] \tag{11}$$

Figure 3a shows the input test image used in the computer simulation. It contains several qualitative human bodies in different positions, rectangles, a pet and small squares simulating small pets. Figure 3b shows the phase distributions of equation 11 multiplied by the phase distribution of a conventional lens. Figure 3c shows the corresponding output image. One can note from figure 3c that images of the human bodies have higher brightness if compared to the images of all other features.

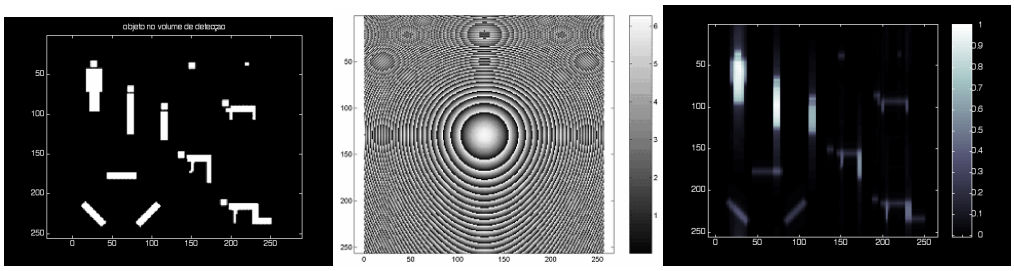

(a) **(b)** **(c)**

Figure 3: (a) Input test image used in the computer simulation. It contains several qualitative human bodies in different positions, rectangles, a pet and small squares simulating small pets; (b) resulting Fresnel lens with spatial filtering; (c) the corresponding output image. One can note that images of the human bodies have higher brightness if compared to the images of all other features

Conclusions

In this work we describe the wavefront coding method applied to passive infrared motion sensors. The new proposed lenses have the ability to distinguish the presence of humans from pets. The lenses are designed considering a cubic phase distribution. The cubic phase distribution generates invariant intermediate images over large region of focus. This aberration control allows a high tolerance in the fabrication of the lenses and in the alignment errors of the sensor. We verified the behavior of the cubic phase mask in one-dimensional systems, testing this distribution in the vertical direction. We simulated several qualitative human bodies in different positions, as well as other features, such as small pets. As a result, we demonstrated that the proposed system is able to enhance the information of vertical features, making possible, in this way, the distinction of the presence of humans from pets.

Acknowledgements

The authors would like to thank FAPESP for financial support.

References

1. US patents: 4.052.616 (1977), 4.321.594 (1982), 4.535.240 (1985).
2. Edward R. Dowski, Jr., and W. Thomas Cathey "Extended depth of field through wave-front coding" *Applied Optics*, **34 (11)**, 1859-1866, 1995.
3. Dowski, E. R. Jr. and Johnson, G. "Marrying optics & electronics: Aspheric optical components improve depth of field for imaging systems", *OE Magazine*, **2 (1)**, 42-43, 2002.
4. US patents: 5.748.371 (1998), 6.069.738 (2000).
5. Dowski, E. R. Jr.; Cathey, W.T.; van der Gracht, J. "Aberration Invariant Optical/Digital Incoherent optical Systems", Publication of the Imaging System Laboratory Department of Electrical Engineering, University of Colorado, Boulder, available (18/07/02) at: http://www.colorado.edu/isl/papers/aberrinv.pdf
6. Cathey, W. T.; Dowski, E. R.; and Alan R. FitzGerrell, A. R. "Optical/Digital Aberration Control in Incoherent Optical Systems" Publication of the Imaging System Laboratory, Department of Electrical Engineering, University of Colorado, Boulder, available (18/07/02) at: http://www.colorado.edu/isl/papers/aberration/paper.html
7. Wach, H.B., Cathey, W. T.and Dowski, E. R "Control of Chromatic Focal Shift Through Wavefront Coding" Publication of the Imaging System Laboratory Department of Electrical Engineering, University of Colorado, Boulder, available (18/07/02) at: http://www.colorado.edu/isl/papers/chromaberr.pdf
8. Joseph W. Goodman. "*Introduction to Fourier Optics*", pp.137, McGraw-Hill Publishing Company, Second Edition, New York, 1996.